We are IntechOpen, the world's leading publisher of Open Access books Built by scientists, for scientists

4,800
Open access books available

122,000
International authors and editors

135M
Downloads

Our authors are among the

154
Countries delivered to

TOP 1%
most cited scientists

12.2%
Contributors from top 500 universities

CLARIVATE ANALYTICS BOOK CITATION INDEX INDEXED

WEB OF SCIENCE™

Selection of our books indexed in the Book Citation Index in Web of Science™ Core Collection (BKCI)

Interested in publishing with us?
Contact book.department@intechopen.com

Numbers displayed above are based on latest data collected.
For more information visit www.intechopen.com

Chapter 6

InSAR Coherence and Intensity Changes Detection

Damien Closson and Nada Milisavljevic

Additional information is available at the end of the chapter

http://dx.doi.org/10.5772/65779

Abstract

This research aims at differentiating human-induced effects over the landscape from the natural ones by exploiting a combination of amplitude and phase changes in satellite radar images. At a first step, ERS and Envisat data stacks are processed using COS software developed by the company SARMAP. Various features related to amplitude and phase as well as to their changes are then extracted from images of the same sensor. Combinations of the features extracted from one image, from several images of one sensor as well as from different sensors are performed to derive robust indicators of potential human-related changes. Finally, possibilities of exploiting and integrating other types of information sources such as various reports, maps, historical or agricultural data, etc. in the combination process are analyzed to improve the obtained results. The outcomes are used to evaluate the potential of this method applied to Sentinel-1 images.

Keywords: minefields, suspected hazardous areas, InSAR, coherence

1. Introduction

In postconflict regions, before the starting of demining operations, investigators have to carry out studies to delineate suspected hazardous areas (SHA). Many factors limit the reliability of their assessments: imprecision of the minefields records in military documents; inaccessibility and impassability of the field; lack of accidental records; inability to accurately position on a map the military units, their actions, confrontations, and the minefields' deployment; etc. Inaccuracies and imprecisions become even worse when dealing with unexploded ordnance (UXO). As a consequence, a significant difference exists between the surfaces to be cleared and the actually mined ones. This situation leads to a waste of time, work, and funds while donations are limited.

1.1. Problem statement

How to refine the delineation of SHA and thus reduce significantly the cost of clearing operations? When conflicts end, the economic activities restart for the benefit of the society but landmines and UXO disrupt this process. When activities take place in former battle zones, the daily works that shape the landscape such as plowing fields, pruning trees, grazing activities, and roads maintenance, etc., are becoming surviving "experiments" for both humans and animals. In regions affected by mines during a long period of time, inhabitants have progressively developed mental SHA maps based on their habituation of the danger.

When correctly located, the inventory of accidents and detonations are primary sources of information to delineate SHA. But the intersection of all inhabitants' mental SHA maps should provide another valuable independent source of information to highlight no man's lands that could be minefields.

Mental SHA maps are only partially exploited by the National Mines Action Centers in charge of the surveys because of the great difficulty to collect all the data. Nowadays, social media can improve the collection of pertinent information but only where the Internet is accessible.

Our research is dedicated to find out a way to use the surviving "experiments" for both humans and animals with radar remote sensing techniques. The working hypothesis/approach is based on the fact that in particular circumstances, and for a specific timespan, all the anthropogenic modifications of a given landscape can be accurately mapped from space-borne radar single look complex (SLC) images owing to the exploitation of the coherence information (e.g., [1] and references therein). The technique based on radar coherence images is known as coherent change detection (CCD).

1.2. Preliminary researches and results: setting up of a relationship between suspected hazardous areas boundaries and interferometric coherence

Since the launch of the first two European remote sensing (ERS) radar satellites in 1991 and 1995, the value of interfermetric synthetic aperture radar (InSAR) coherence images computed from the processing of two SAR scenes, have been recognized as a useful information source for environmental studies [2].

In SAR CCD techniques, the phases of two SAR images of the same scene are interfered. The images must be acquired in the same conditions, i.e., the same incidence angle but with a position slightly different (from a few meters to a few hundred meters). The coherence between two SAR images expresses the similarity of the radar reflection between them. Any changes in the complex reflectivity function of the scene are manifested as a decorrelation in the phase of the appropriate pixels between the two images. In this manner, even very subtle changes in the scene from one image to the next can be detected. In other words, in a given pixel, if the reflection and/or dielectric properties have changed between the two acquisitions, the coherence value of that target is reduced and the accuracy over the distance measurement between the antenna and the ground decreases.

This ability to detect and to localize very subtle changes can be used in demining operations to map human and animals activities during a specific time laps, e.g., 35 days for ERS and Envisat satellites. One of the challenges is to classify the observed changes into two main categories: pertinent or not for the delineation of minefields perimeter.

Whatever, the thematic concerned, since 1991; space-borne radar interferometry techniques were successfully applied all around the world. A large number of InSAR results were obtained over cities, and in warm or cold desert areas (e.g, Landers earthquake dislocation pattern; Shiraz glacier displacements field, etc.). This is due to the fact that such environments/landscapes present surface characteristics that match with the most important InSAR condition of application: the preservation of the phase coherence through time.

Pioneering researches conducted in semiarid to hyperarid regions [3–8] showed that radar coherence images were able to bring useful insights for geomorphology, geology, soil moisture, and erosion phenomena. Among them, a few suggested the unique function of coherence imagery as a tool for monitoring environmental impacts of human activities [6, 9–11].

In the 2000s, first experiments were conducted at the Space Centre of Liege, and then extended at the Signal and Image Centre (see **Figure 1** and **Figure 2**) demonstrated the CCD capability for discrimination between topsoil disturbed or not by anthropogenic/animal activities. The areas of interest were centered over the Dead Sea region.

Later on, based on the knowledge gained through projects financed by the Ministry of Defense, other experiments related to Surface-to-Air Missile sites and military airfields [12, 13] have shown that the CCD technique is able to develop a persistent picture of activities within an area of interest and allows the delineation of the system of fortification, even if hidden by camouflage. In the frame of security applications, CCD is particularly interesting in the surveillance (**Figure 3**) and the detection of intrusions.

CCD technique is less efficient in places where too many human activities occur, or in zones where the substratum is too hard to record detectable surface modifications (such as in urban areas). Seasonal variations can affect significantly the estimated coherence, both in terms of overall average value (weather dependence) and in localized natural effects (e.g., vegetation, steams, and water bodies with seasonal variations). Additional information has to be exploited to carefully analyze and understand the nature of the difference coherence losses.

1.3. First hint to delineate mental suspected hazardous areas

The very first observation of a minefield with CCD was derived from ERS spaceborne radar images processed in the frame of a study dedicated to active faulting in the Dead Sea region [14]. Interpretation of interferograms and coherence images led to the first delineation of a square kilometer-size minefield in the northern part of the terminal lake (**Figure 1**). The preservation of phase coherence through time in a zone that normally should have lost coherence provided the first hints to delineate “mental SHA”.

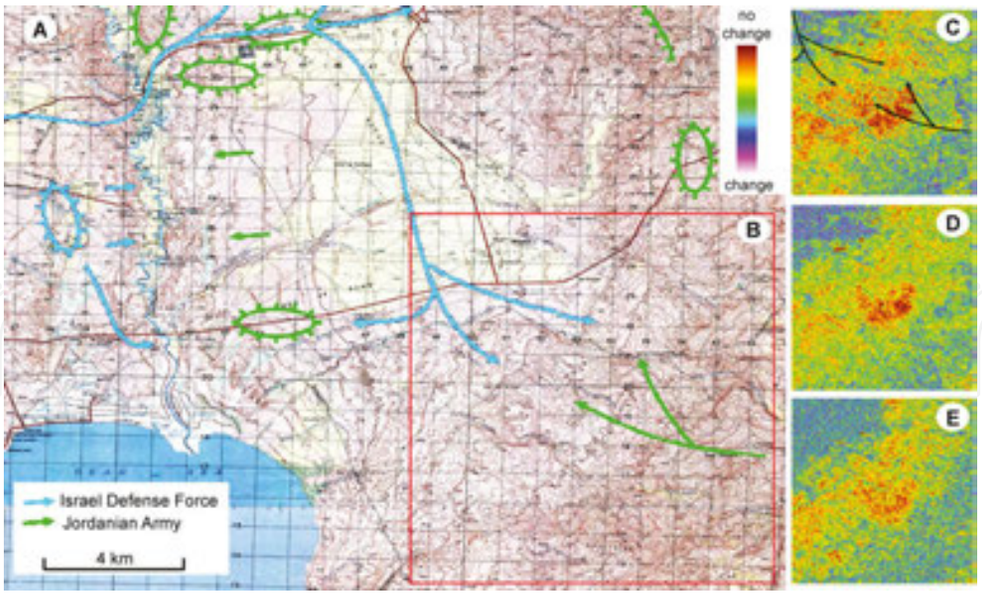

Figure 1. (A) Israel Defense Force and Jordanian army troops' movements during the battle of Al-Karamah 21 March 1968, background 1:50,000 map of Karama, Sheet 3153 IV, series K737 (USA). (B) Location of insets C, D, and E. (C) Interferometric coherence (pixels 20 m), 1995-07-30 and 1995-11-12, temporal baseline = 105 days, perpendicular baseline = 304 m, descending path. Black arrows correspond to Israeli and Jordanian troops' movements. (D) Interferometric coherence, 1995-07-30 and 1996-07-14, temporal baseline = 350 days, perpendicular baseline = 57 m, descending path. (E) Interferometric coherence, 1995-12-16 and 1999-05-29, temporal baseline = 1260 days, perpendicular baseline = 92 m, ascending path. The color palette ranges from change (loss of coherence or surface modifications) to no change.

Figure 1(A) describe some actions of the Al-Karamah battle fought on March 21, 1968, between the Israel Defense Forces and the Jordanian Army. Before and during the battle, minefields were laid and then progressively cleared in the next decades. Systematic demining operations took place only after the Oslo Accords in 1993–1994. Ten years later, at the Space Center of Liege, ERS satellite data acquired from 30/07/1995 to 29/05/1999 were processed to generate differential interferograms and their associated coherence images. Unexpected high coherence values were noticed on the foothills of the Dead Sea basin (**Figure 1B**), Jordanian side. In 2002, during a field survey, rusty barbed wires and warning signs revealed a former battlefield. Farmers and shepherds indicated that the plateau was cleared in 1999 in anticipation of the Pope John Paul II coming in the area (March 20–26, 2000). Indeed, to shorten the trip between Mount Nebo and the Baptism Center next to the Jordan River, the government of Jordan created one new road that had to cross the minefield. Based on these elements, it was deduced that the coherence preservation was a consequence of the absence/presence of grazing activities. Since the Al-Karamah battle, Bedouins had modified their itineraries to protect their flocks and themselves.

In **Figure 1(C)–(E)**, colored coherence images show the presence/absence of perturbation of ground scatterers between two acquisition dates. Coherence images having different time spans (C = 105, D = 350, E = 1260 days) do not display exactly the same amount of changes. Depending on the environmental conditions and land use dynamics, a kind of "decantation process" is necessary to distinguish permanent boundaries of untouched zones (e.g., comparison between **Figure 1C** and **E**).

http://dx.doi.org/10.5772/65779

Based on the previous reasoning, the linear minefield along the Jordanian-Syrian border was mapped with a pair of ERS images acquired 70 days apart (**Figure 2**). The borderline crosses a wide cropped and pastured plateau where coherence is lost rapidly. On the contrary, the no man's land between Syria and Jordan is not affected by human activities and appears highly coherent. Elsewhere over the scene, coherence is preserved on the rocky zones (**Figure 2**, clouds of brown spots). Coherence images do not map minefields but no man's lands in which landmines can be present (**Figure 2B–D**) taking into account the context.

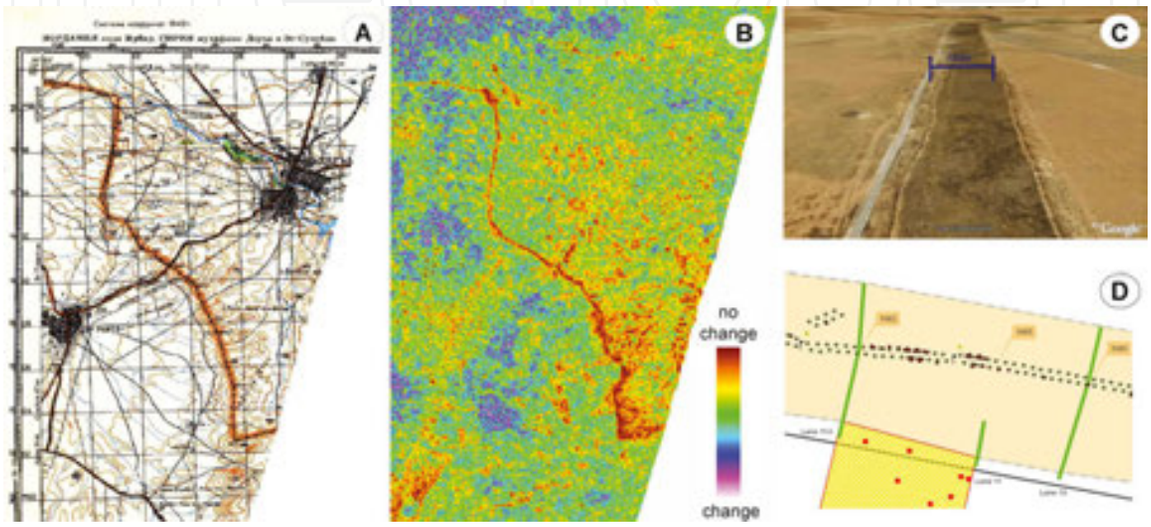

Figure 2. No man's land mapping with ERS coherence image, Jordan-Syria border. (A) 1:100,000 Sheet 9-37-121 (USSR) – graticule 2 km - Irbid, Jordan, is on the left. (B) Interferometric coherence (pixels 20 m), 1995-07-29 and 1995-10-07, temporal baseline = 70 days; perpendicular baseline = 148 m. (C) Birdseye view of the 100 m wide no man's land located over the border (© Google Earth). (D) mines' location into the no man's land (© Norwegian People Aid).

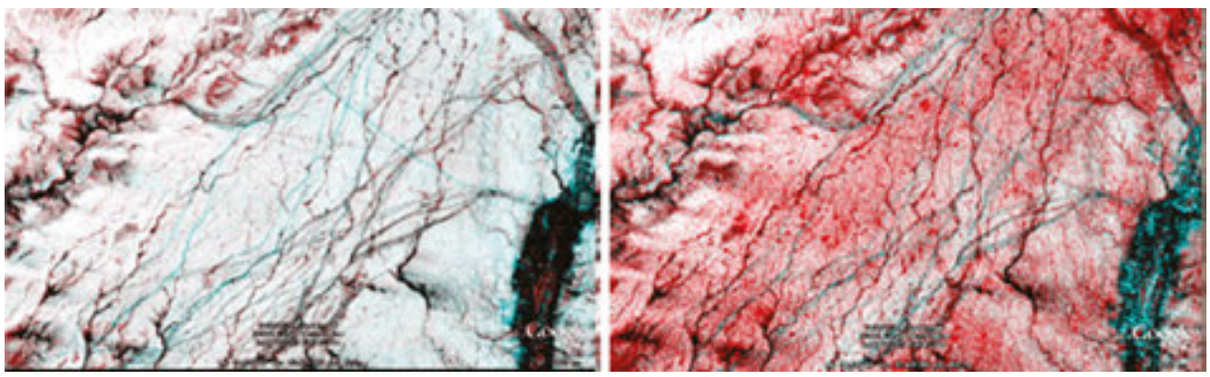

Figure 3. Color composites of a sequence of coherence images derived from Envisat data over an area in Afghanistan. The following coherence combinations are used: 1 – (2004.04.28 – 2004.08.11), 2 – (2004.08.11–2004.11.24), 3 – (2004.11.24–2005.03.09), 4 – (2005.03.09 – 2005.04.13). Left image: 1 – red, 2 – green, 3 – blue. Right image: 4 – red, 2 – green, 3 – blue. Images processed by SARMAP SA.

In 2011, in collaboration with the private company SARMAP, another test was realized in a desert plain, Kandahar region, Afghanistan. The objective concerned the capability

of discrimination between ephemeral streams and traces of convoys from a coherence images stack. **Figure 3** compares two color composites created from a sequence of five Envisat ASAR scenes. Natural decorrelation effects can be identified like seasonal and permanent traffic roads as well as seasonal torrents and permanent rivers.

1.4. Purpose of this chapter

Figure 1–3 describe a CCD approach based on a dataset ranging from two to five SLC images. The environmental conditions of applicability are favorable. Considering these preliminary but promising results, a research project untitled SPaceborne Radar INterferometric Techniques for Humanitarian Demining Land Release (SPRINT) [15] was proposed to test and evaluate an approach for SHA area reduction in Croatia based on coherence and intensity images analysis and interpretation. The project was financed by the Belgium Scientific Policy (BELSPO). It received the support of the European Commission TIRAMISU project, and of the private company SARMAP that provided radar images from the European Space Agency and the outputs of the SBAS processing (see below) with their software Sarscape™.

The project idea consisted in processing ERS and Envisat stacked images to generate time series geocoded coherence and intensity data, and then fusing this multitemporal information to map changes in known SHA. It was expected that the types of change and their spatial extension could provide additional inputs in the Decision Support System to reduce the size of the SHA.

In this chapter the main outcomes of this research are presented. The following three scientific questions are addressed as well:

1. Is it useful for SHA area reduction to use InSAR stacking techniques to produce time series of intensity and coherence images of minefields (Gospić, Croatia)?
2. What kind of fusion analysis do we have to perform to extract relevant changes for area reduction?
3. Does it make sense to collect regularly Sentinel-1 radar images over a war zone or a postconflict region to exploit these data with stacking techniques in humanitarian demining?

2. Method

At a first step, C-band ERS and Envisat image stacks are processed using PS-SBAS (permanent scatterer and small baseline) tools developed by the Swiss company SARMAP (Sarscape™ software). Detailed information is provided below. In a next step, unsupervised classification based on the analysis of temporal signatures is performed within each of the stacks of ERS amplitude data, ERS coherence data, Envisat amplitude data, and Envisat coherence data, separately. After that, combination of the obtained results is performed. Validation process is discussed after the presentation of the results.

http://dx.doi.org/10.5772/65779

2.1. Change detection with spaceborne radar

The radar antenna on board satellites transmits a coherent signal that is backscattered by the Earth surface before being detected by the same antenna. A SAR signal is complex. Each pixel of an image holds intensity and phase information. The intensity depends on the ground roughness, the soil moisture, and the incidence angle. The phase information, expressed as an angle, depends on the optical path travelled by the radar wave along its round trip.

Change detection is an application for which SAR is particularly well suited as this type of sensors can consistently produce high-quality well-calibrated imagery with good geo-location accuracy. Two forms of change detection in repeat-pass SAR imagery may be considered, namely coherent and incoherent change detection:

1. Incoherent change detection (ICD) identifies changes in the mean backscatter power of two scenes by comparing sample estimates of the mean backscatter power taken from the repeat-pass image pair. Typically, the sample estimates are obtained by spatially averaging the image pixel intensities (amplitude squared) over local regions in the image pair. The mean backscatter power of a scene is determined by the structural and dielectric properties of the scene, and thus may be used to detect changes in soil or vegetation moisture content or surface roughness.

2. Coherent change detection (CCD) compares the phase of two images for inconsistencies. To detect whether or not a change has occurred, two images are taken of the same scene with a same incident angle, but at different times. These images are then geometrically registered so that the same target pixels in each image align. After the images are registered, they are checked pixel by pixel. Where a change has not occurred between the two images, the pixels remain the same. When the pixels are different, a change has occurred.

Both methods are useful for detecting changes, but they do not measure their magnitude. One of the major issues is defining what "relevant" changes are. By combining the results with ancillary data owing to data fusion techniques, it is possible to improve the detection quality and reliability as well as to differentiate well between changes. Therefore, the SPRINT project was centered over a sequence of activities dedicated:

1. To process and geocode large amount of space-borne radar data, originally, from ERS and Envisat (C-band).

2. To extract anomalies, land-cover types, etc., according to the information available.

3. To fuse, at different levels (feature and/or decision level), various pieces of information coming from one image (in order to improve the quality of the result) as well as change detection results obtained from different sources (images of one sensor or of different sensors).

4. To include existing contextual information, experts opinions, and other knowledge sources in the fusion process and to assess the influence of their inclusion on the final result.

5. To perform qualitative and quantitative assessments of the assets and drawbacks of each radar interferometric techniques as well as of each sensor combination, for dedicated tasks, in specific environment under surveillance, to support future land release actions.

2.2. InSAR processing

SAR repeat pass interferometry is based on two images acquisitions of the same area from slightly displaced orbits of the satellite. The ERS and Envisat repeat pass periods are 35 days but when ERS 1 and 2 were orbiting together (1995–1999), a place was revisited one day apart ("ERS tandem pairs").

During the processing, both images are coregistered ("slave" image over "master" one). In CCD, the phase differences are calculated leading to the so-called interferograms. These interferograms contain information related to local elevation, local displacement, and noise. This noise, or phase decorrelation, records the slight changes in scatterers distribution on the observed Earth surface between the two acquisitions.

There are three "interferometric products" from two SAR scenes. They can be displayed either in radar geometry (slant range) or geocoded:

1. An intensity image that helps to locate points of interest. The radar cross-section of a scatterer is calculated from the ratio of the power density received by the scatterer to the backscattered power density.
2. A phase difference image or interferogram with either only the orbital contribution removed (to show the topographic contribution) or with both orbital and topographic contributions removed (to show ground displacements and phase noise).
3. A coherence image that presents the confidence level of each pixel in the phase difference image.

Coherence (equation 1) refers to a fixed relationship between waves in a beam of electromagnetic radiation. Two wave trains are "coherent" when they are in phase. In SAR interferometry, coherence is used to describe systems that preserve the phase of the received signal. Coherence value can be estimated by means of the "local coherence" of an interferometric SAR image pair. The local coherence estimator is the cross-correlation coefficient of the couple estimated on a small window [16, 17]:

$$\gamma \tilde{=} \frac{\left|\sum_{i=1}^{L}\sum_{j=1}^{M} \mathrm{Im}_1\left(x_i, z_j\right)\mathrm{Im}_2^*\left(x_i, z_j\right)\right|}{\sqrt{\sum_{i=1}^{L}\sum_{j=1}^{M}\left|\mathrm{Im}_1\left(x_i, z_j\right)\right|^2 \sum_{i=1}^{L}\sum_{j=1}^{M}\left|\mathrm{Im}_2\left(x_i, z_j\right)\right|^2}} \quad (1)$$

where Im_1 is the complex signal of the "master" image and Im^*_2 is the complex signal in the "slave" one. The coherence of a pixel is estimated by the means of kernels with $L \times M$ pixels. In an interferogram, the coherence ranges from 0.0 (total decorrelation, the interferometric

phase is pure noise) to 1.0 (phase correlation is preserved). As a statistical value, it cannot provide quantitative measurements of the ground scatterers disturbances. However, a physical interpretation is that it represents the fraction of power scattered by unchanged parts of the scene [18]. The coherence image serves as a measure of the quality of an interferogram and gives information about the surface type (e.g., vegetated versus soil and rock) or shows when a tiny, otherwise invisible change has occurred in the image. Coherence imagery is able to detect centimeter scale changes in the scatterers distribution.

The coherence values are affected by:

1. The local slope (steep slopes oriented toward the satellite line of sight lead to low coherence).
2. The properties of the surface being imaged (e.g., vegetated or water surfaces have low coherence).
3. The time span between the passes in an interferogram. Long lags lead to higher variations in scatterers distribution and hence to lower coherence.
4. The baseline, which is the distance between the satellites positions. The perpendicular component is what matters for coherence purposes. Generally, the optimal baseline length is between 0 and 400 m (large baselines lead to low coherence).
5. The poor coregistration, i.e., the process of lining up two images, a "master" and "slave", covering the same area in a way that they fit exactly on top of each other.
6. The poor resampling leads to low coherence during the InSAR processing [19, 20].

2.3. Advanced InSAR processing

Interferometric stacking techniques emerged in the last decade as methods to obtain very precise measurements of terrain displacements, and in particular of subsidence phenomena. The so-called Persistent Scatterers (PS) [21] and Small BASeline (SBAS) [22] methods can be considered as the two most representative stacking approaches.

In both cases, the exploitation of 20 or more satellite saynthetic aperture radar (SAR) acquisitions obtained from the same satellite sensor with similar geometries on the area of interest allows to measure displacements with an accuracy in the order of few mm/year, and to derive the full location history of " coherent pixels with an accuracy of 1 cm or better for every available date.

The "area-based SBAS-like" tool of Sarscape™ Interferometric Stacking Module is dedicated to compute mm-scale displacements on distributed targets. Geocoded coherence and intensity images are side-products. Therefore, the procedure stopped once the information needed was available.

The first step consisted in the connection graph generation to define the ensemble of pairs to process. These pairs were displayed as connections in a network that links each acquisition to others. Given N acquisitions, the number of maximum theoretical available connections is

(N*(N − 1))/2. The connection graph generation tool permitted to choose the most *a priori* reliable connections.

One acquisition considered as Super Master was automatically chosen among the input acquisitions. The Super Master is the reference image of the whole processing and all the processed slant range pairs were coregistered on this reference geometry.

Then, from these pairs, the "Interferometric Workflow" and the "Refinement and Re-Flattening" tools generated a time series of geocoded coherence and intensity images.

3. Material: training areas and image datasets

In 2008–2010, the Croatian Mine Action Center (CROMAC) successfully tested an Advanced Intelligence-Decision Support System (AI-DSS) over three communities (Gospić, Bilje, and Drniš) to improve SHA circumscription process [23]. In SPRINT, the documented Gospić area was used to test and evaluate a contribution based on the processing of ERS and Envisat satellite radar images time series.

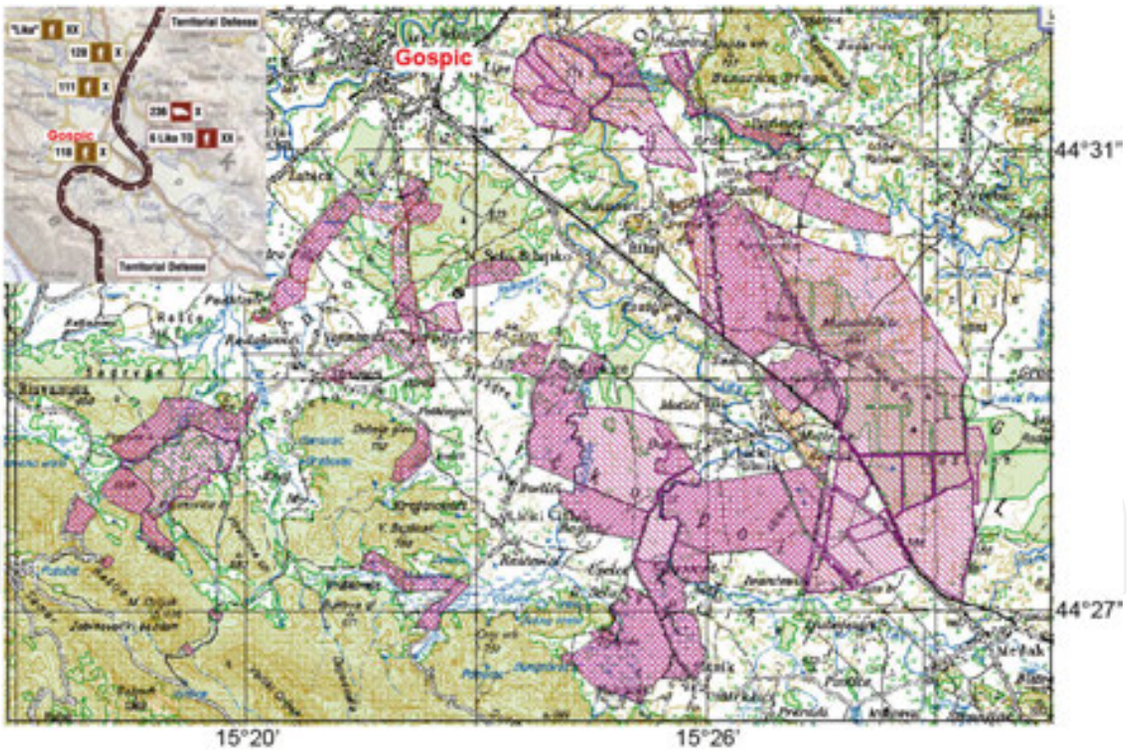

Figure 4. Several battles took place in the Gospić salients from 1991 to 1995 (inset). Minefields are located in a bulge of the front line. Suspected hazardous and confirmed hazardous areas are shown respectively in hatched and crosshatched purple polygons (2009 situation) over a 1:50,000 topographic map, graticule 4 km. Source: Milan Bajic.

The plain of Gospić (**Figure 4**) is characterized by environmental conditions less favorable than those of Jordan or Afghanistan (**Figures 1–3**) because of the forest covering the valley sides

(volume decorrelation), the escarpment of the valley sides (shadows; layover), and the climatic conditions (moisture decorrelation).

Apart from these drawbacks, SPRINT demonstrated the possibility to process data and get valuable results for the analysts. The well-documented minefields allowed the study to be carried out in three main steps, without expensive and time consuming field surveys: data acquisition and processing, data fusion, and validation inside a geographical information system.

In the geographical information system ArcGIS™, the geocoded coherence and intensity images (100 ×100 km) have been clipped with confirmed hazardous areas displayed in **Figure 4** (crosshatched). A 300 m wide buffer was also created to compare the results in the minefields with the ones in the immediate vicinity.

Two major datasets were created from radar images (**Table 1**): "minefields" and "buffers". For each one, ERS and Envisat intensity and coherence were computed. SARMAP collected radar images from the archives of the European Space Agency. Sarscape™ Focusing Module generated single look complex images based on a ω-κ frequency domain algorithm. Two stacks of 42 ERS SLC images (1992/08/01–2009/06/02) and of 40 Envisat scenes (2002/11/07–2010/10/21) were the inputs of SBAS processing.

Satellite images track 315 – frame 873 (ascending)	**42 ERS intensity**	**112 ERS coherence**	**40 Envisat intensity**	**127 Envisat coherence**
26 minefields	1092 subsets	2912 subsets	1040 subsets	3302 subsets
26 buffer zones	1092 subsets	2912 subsets	1040 subsets	3302 subsets

The number of coherence image is higher than the one of the intensity because SBAS process multiple pairs of images

Table 1. Image dataset processed and analyzed in SPRINT.

Although both radar sensors are using C-band, the interferometric combination of Envisat and ERS data was not performed because the interferometric phase is strongly dependent on the radar frequency. The radar center frequency of Envisat (5.331 GHz) is slightly different compared to the ERS sensor (5.300 GHz). The difference of 31 MHz prevented the simple combination.

4. Results

Figure 5 locates 26 polygons corresponding to the confirmed hazardous areas over a visible satellite image (ArcGIS "world image" layer) to illustrate the land use/land cover. Most of the polygons are located in a plain extending ESE from Gospić. Agricultural parcels, pasture lands, and a few woodlots cover most of the flatten zones. The southern part is hilly and forested.

Figure 5. Location of the confirmed hazardous areas in the plain of Gospić. The minefield in light blue color is used to illustrate the whole process from the intensity and coherence images to the indicators of potential human-related change map.

In terms of land use/land cover dynamics, the comparison between Landsat images acquired from 1993 to 2015 indicated that the landscape is very stable and that most minefields are either covered by woodlots or pasture lands. A very little number presented evidence of agricultural activities.

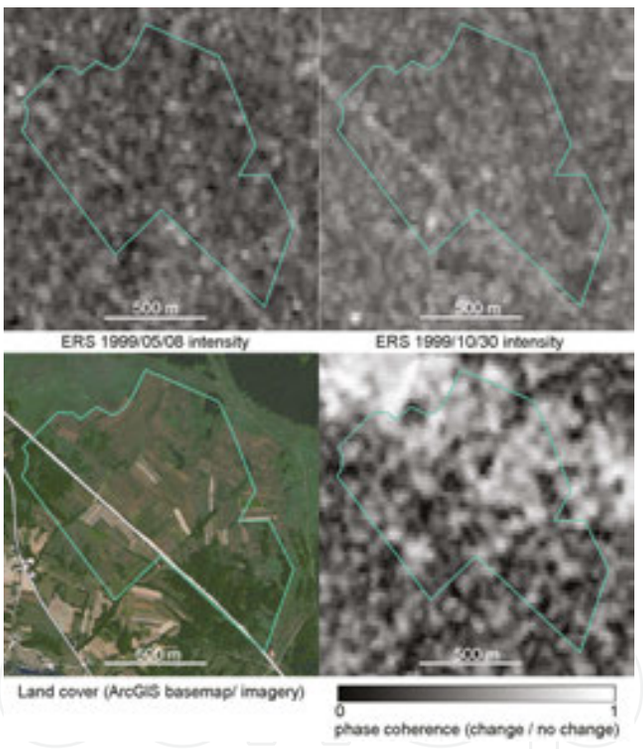

Figure 6. Comparison between intensity and coherence data with the visible information. Radar images have been processed with a pixel size of 25 m.

The wide polygon in **Figure 6** is an illustrative case study. This minefield is almost flat and covered by woods, pastures, and crops. A main road also crosses the area. The landscape displayed in radar image is very different than the one obtained in the visible wavelength because the physical mechanism used to create those scenes is completely different. Radar and visible data are independent, reliable, and complementary sources of information. However, at a first glance, radar data provide no information directly useful in demining operations. In

http://dx.doi.org/10.5772/65779

the intensity images the main road crossing the polygon can be distinguished but its width is overestimated. The limits between woods, crops, and pastures cannot be observed. Coherence displayed in gray-scale provides information on the ground scatterers' perturbations between two dates (1999/08/05–1999/10/30). However, radar intensity and phase provide information complementary to the visible ones about the subtle changes of the ground surface.

4.1. Natural decorrelation revealed by ERS tandem pairs

As previously mentioned, slopes, forests, and high moisture zones are able to decorrelate the signal in less than one day. Hence, in those zones, it is clearly impossible to work with radar time series. **Figure 7** illustrates this important element for the approach to delineate SHA perimeters. The inset on the right side shows the land cover of the minefield during the period of war (1991–1995). Green color indicates wooden areas. The main road crossing the zone already existed and appears as a NW-SE linear light grey color feature.

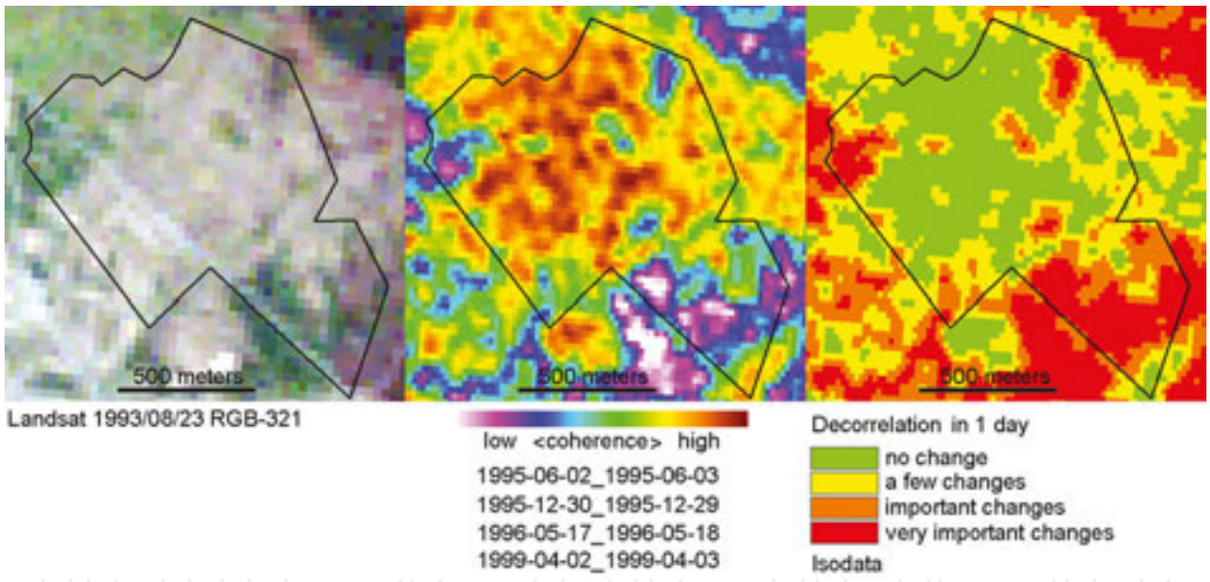

Figure 7. Evaluation of the decorrelation phenomena from tandem pairs (temporal baseline = 1 day). Green and yellow areas allow performing time series analysis. The orange red areas loose very quickly coherence. No information can be retrieved.

The middle inset is the average coherence between the four tandem pairs. The coherence is generally well preserved everywhere in the polygon at the noticeable exception of the wooden parcels. The left inset is a classification of the previous data in four classes (unsupervised). The green color shows where further studies can be conducted while the red color indicates that no information can be retrieved. Orange and yellow colors are areas where studies can be conducted but the environmental conditions are less favorable. In yellow spaces there are still certain levels of confidence that can be obtained.

4.2. Data fusion first level

Elementary pieces of information (intensity and coherence), such as the ones displayed in **Figure 6**, become relevant once exploited through stacks of data. Four data sources have been used (**Table 2**): ERS coherence, Envisat coherence, ERS intensity, and Envisat intensity.

Satellite images track 315 – frame 873 (ascending)	**112 ERS coherence**	**127 Envisat coherence**	**42 ERS intensity**	**40 Envisat intensity**
Figure 6′ Minefield	112 subsets	127 subsets	42 subsets	40 subsets
Unsupervised classification				

Table 2. Unsupervised classification results.

Data within each of these stacks have been combined and classified using multitemporal signature analysis, where pixels with similar signatures are grouped together. The output is an unsupervised classification of ERS coherence, ERS intensity, Envisat coherence, and Envisat intensity. These classification results are inputs for the second level.

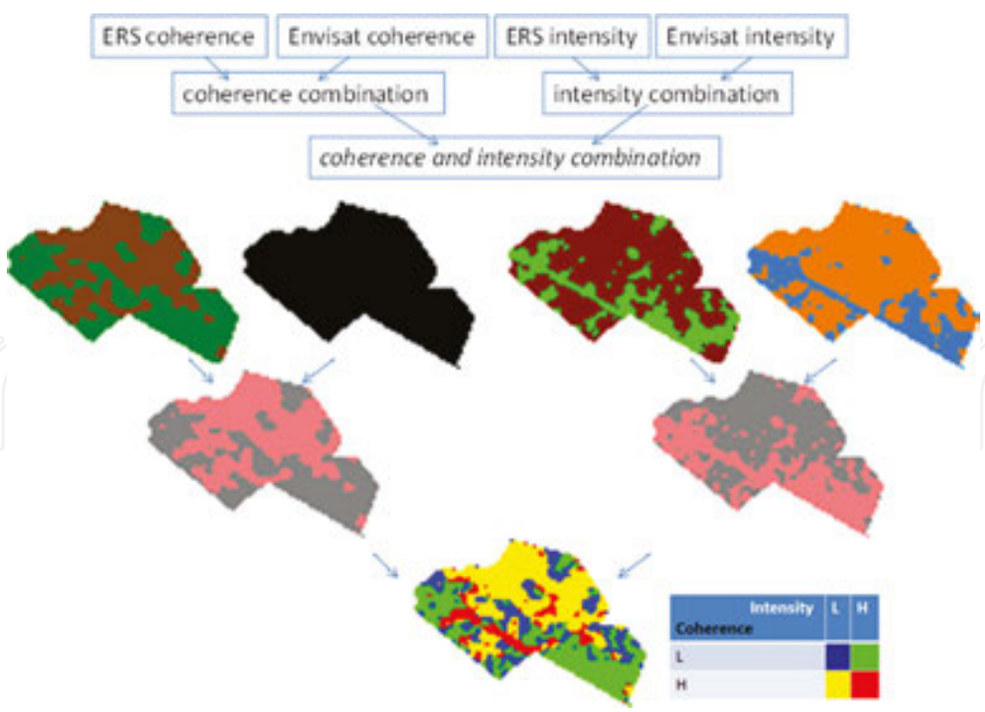

Figure 8. Example of combination, coherence classification results of Envisat and of ERS and intensity classification results of Envisat and of ERS. Then, fusing the two intermediate fusion results to create a map of indicators of potential human-related changes in the landscape. L = low; H = high.

http://dx.doi.org/10.5772/65779

4.3. Data fusion second level

The combination is performed using different strategies:

1. Fusing firstly coherence classification results of Envisat and of ERS, and intensity classification results of Envisat and of ERS. Then, fusing the two intermediate fusion results (**Figure 8**).
2. Fusing first the two ERS results (coherence classification and amplitude classification), and the two Envisat results (coherence classification and amplitude classification), and then fusing the two intermediate results (**Figure 9**).

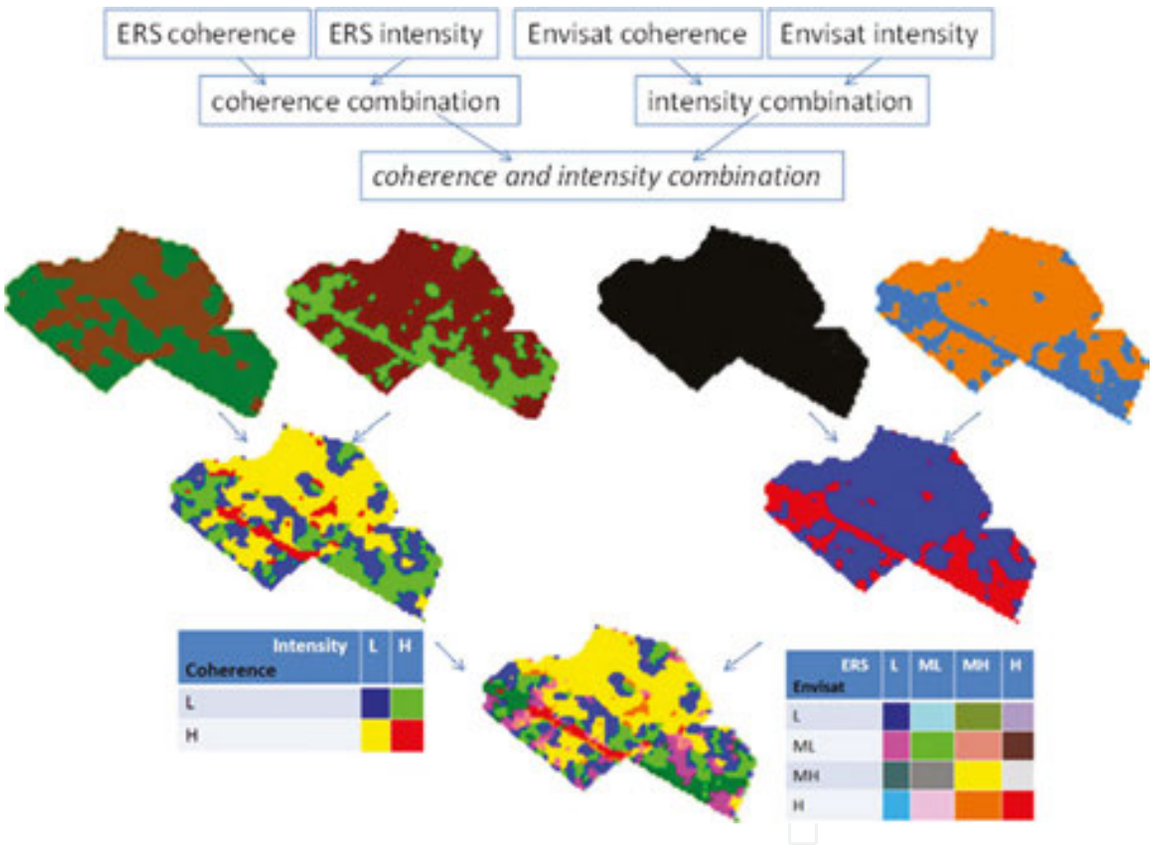

Figure 9. Example of combination, coherence classification results and intensity classification results of Envisat of ERS are combined. Then, fusing the two intermediate fusion results to create a map of indicators of potential human-related changes in the landscape. L = low; ML mean low; MH mean high; H = high.

The two strategies should provide the same final result only if the combination operators are commutative and associative. It is not the case here since different reasoning is applied in function of the data to be fused. The fusion order matters and influences the final result. The two strategies are developed and tested in parallel in order to cover various situations that might occur in reality (only one sensor used; only amplitude or coherence data available, etc.).

5. Discussion

5.1. Performance evaluation

Taking into account that humanitarian demining is a very sensitive matter, it was not easy to validate on the ground, especially, in the case of a demonstration project due to the lack of time, as well as human and material resources. To validate the results, alternative solutions were taken. One of the validation sources provided by CROMAC was photos as well as various indicators of mine presence and mine absence.

– Indicators of mine presence: destroyed houses, abandoned roads and areas, bunker lines, trenches, cover for infantry and artillery, shallow drafts, bridges.

– Indicators of mine absence: safe roads, houses in use, roads in use, and areas in use.

Although these pieces of knowledge were very informative, they were not geocoded, so it was not possible to use them directly for validation.

Due to their sensitive content, CROMAC could not provide geocoded validation data, so this type of validation had to be left to them.

Thus, the only means to validate the results in SPRINT was to compare them with existing (published) aerial data.

Figure 10 shows a superimposition of ERS classification results over aerial photo of the region of interest. Zones with trees are clearly classified as a class labeled by green color. Agricultural zones are well classified in the class labeled yellow. Roads are in red, and the blue color seems to be the zone around forests and trees. There are various possibilities to explain why this class occurred as a separate class in our classification. For example, it could be due to the acquisition mode itself (radar shadows), or due to works in the bordering zones around trees. A further investigation in this direction, involving potentially the terrain observation, would be necessary.

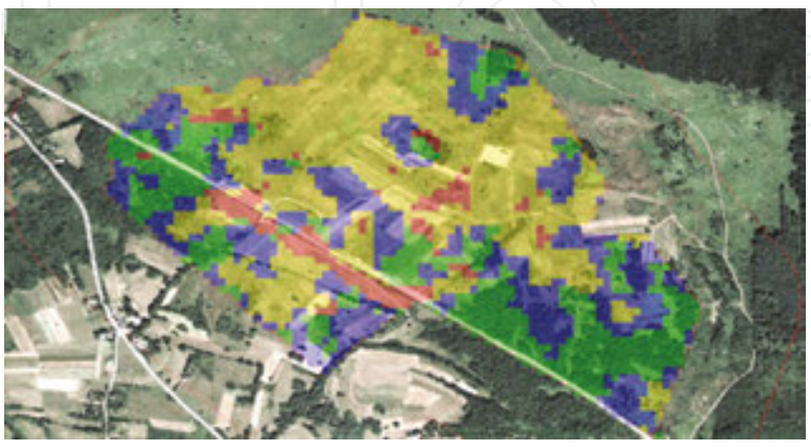

Figure 10. Classification of ERS data over an aerial photograph.

http://dx.doi.org/10.5772/65779

In **Figure 11**, for an easy visual comparison, an aerial image of one of the minefields is given (top left), together with the danger map obtained from CROMAC (top right) and the two classification results at the bottom (ERS left, Envisat right). In the danger map, the level of red indicates the level of danger (more dangerous zones are represented with darker red). Green zones are surfaces in use, while purple corresponds to the roads in use.

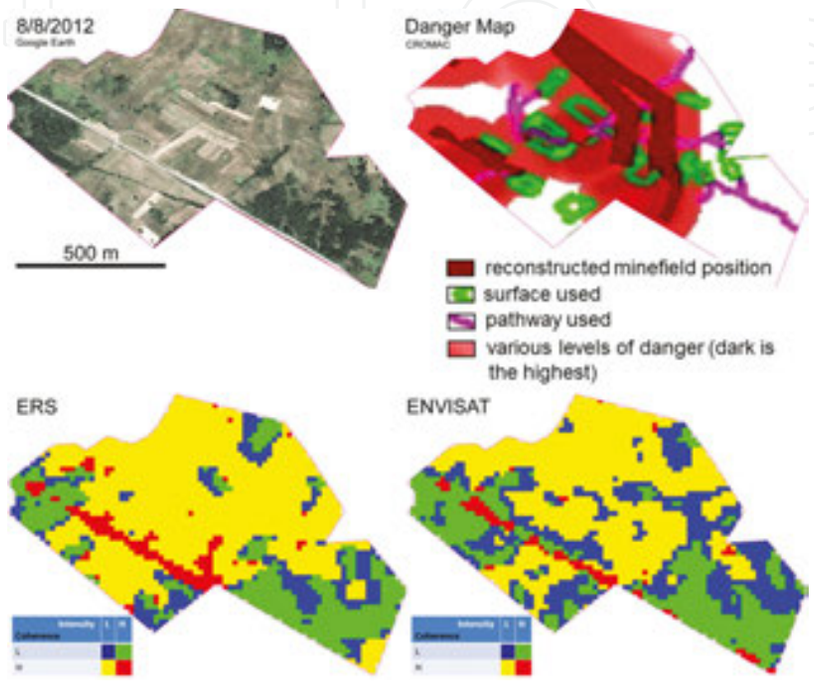

Figure 11. Top: aerial image of one of the regions (left); danger map obtained from CROMAC (right); the color code is: brown = reconstructed minefield position; green = surface used; purple = pathway used; red = various levels of danger (dark is the highest); bottom: ERS classification result (left), Envisat classification result (right).

Based on a visual comparison with the classification results, we can see that fields in use belong to the radar yellow class. Following that logic, we might conclude that the whole yellow classified zone could be suggested to CROMAC as mine-free (in use).

It should be noted that the classification results should be treated as a layer in creating/modifying CROMAC database, and not as a self-sufficient decision-making information, since in creating danger maps, other sources of information should be taken into account as well, that we have not used in our classification, such as: mine laying records, mine accidents, mine incidents, history of battles, etc.

As long as the SPRINT project is concerned, the fact that obtained results are able to distinguish areas in use from forests and other zones and that there is a correspondence with danger maps proves that the method developed in the project is promising.

Taking into account that the terrain itself is not ideal from the point of view of SAR sensors, we might expect even better results for some other areas, where terrain conditions are more beneficial for SAR acquisition (flat zones, not so many trees, etc.—see **Figures 1–3**).

5.2. Research outcomes

When the environmental conditions of applicability are met, to a certain extent, it is possible to apply CCD for the improvement of the SHA delineation (see **Figures 1** and **2**).

CCD techniques present limitations related to the radar interferometric methods. Based on results published in the past 20 years (e.g., [4, 18, 20]), at least nine major factors limit the applicability or the effectiveness:

1. Coherence is a mathematical estimation computed usually with 3 ×3, 5×5, or 7 × 7 windows. The SHA limits are thus fuzzy.
2. Coherence decreases when the perpendicular baseline between acquisitions increases. The use of radar images pairs characterized by short baselines should be favored.
3. Coherence decreases with the angle of local slopes. The interpretation should be confined to flat and undulated surfaces.
4. Coherence is low over vegetation cover (volume scattering) in X-, C-, and L-bands. The approach provides best results in open spaces such as pastured or cropped areas (**Figure 2**).
5. Coherence varies with soil moisture content. Semiarid and arid zones like Iraq or Libya should be preferred.
6. The efficiency of the approach depends on the land-use impact on the ground surface (displacement of the ground scatterers). In desert areas, lot of time can be needed to observe a relevant contrast because of the lack of activities. Coherence remains high most of the time. On the contrary, in busy places, it is possible to detect areas of interest with short temporal baselines (e.g., 35 days for ERS).
7. The ground surfaces must be covered with scatterers able to move when an activity occurs. Hard rock surfaces preserve coherence even when activities occurred. No signal is recorded.
8. Pixel resolution: the smaller the pixel, the longer the coherence is preserved. Indeed, small pixels gather less scatterers than wide pixels. In a small pixel, it is less possible to record an event than in a wider pixel.
9. In time series analysis, the variation of the meteorological conditions through year can affect the efficiency. Regions with relatively stable meteorological conditions will be favored.

Figure 12 presents a qualitative assessment of the approach based on a set of fundamental parameters: human activities, slopes, vegetation cover, and precipitation (climate variable). Up to now, the best results have been obtained in places characterized by human activities modifying the surface the landscape, flat to very gentle slopes, relatively poor vegetation cover, and climate relatively dry to extra dry.

http://dx.doi.org/10.5772/65779

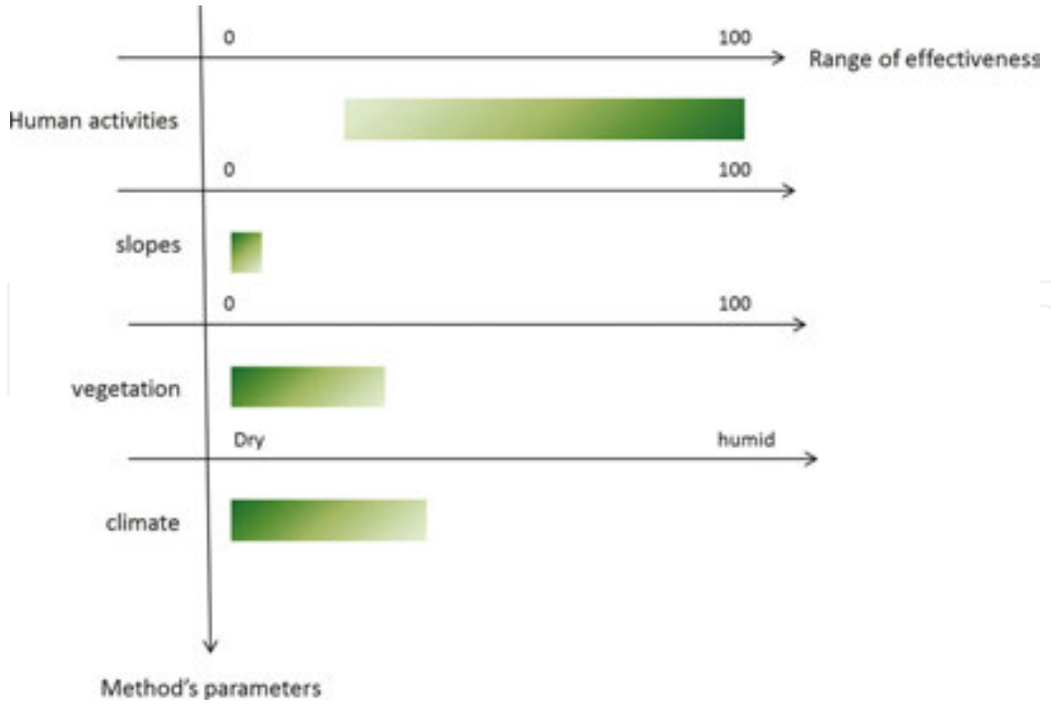

Figure 12. Qualitative assessment of the approach. Effectiveness of the method for C-band datasets. Based on Gospic (Croatia) and Jordan experiments.

6. Conclusion

Is it useful for SHA area reduction to use InSAR stacking techniques to produce time series of intensity and coherence images of minefields (Gospić, Croatia)?

SPRINT demonstrated that valuable information for the mines action centers can be provided through the processing of radar image stacks acquired during and after a conflict. SPRINT used successfully the COS Sarscape™ software and the objectives were achieved. The outputs of the interferometric processing have been successfully manipulated in ArcGIS to generate subset images useful for the fusion analysis step. All outputs, whatever the level in the processing chain, were in a standard format compatible with any types of (open) integrated geospatial systems.

What kind of fusion analysis do we have to perform to extract relevant changes for area reduction?

Unsupervised classification based on the analysis of temporal signatures had been performed within each of the stacks of ERS amplitude data, ERS coherence data, Envisat amplitude data and Envisat coherence data, separately. After that, combination of the obtained results have been performed.

Does it make sense to collect regularly Sentinel-1 radar images over a war zone or a postconflict region to exploit these data with stacking techniques in humanitarian demining?

The answer is positive. Since 2015, a large part of the world is covered by Sentinel-1 SAR (C-band) images. They are for free by the EU-ESA owing to the Copernicus project. The resolution is better than ERS and Envisat (5 vs. 20 m); the revisit time 11 days (and then 6 days when 2 satellites) versus 35 days.

Acknowledgements

This research was funded by the FP7 TIRAMISU project. In particular we wish to thank Dr. Vinciane Lacroix and Prof. Yvan Baudoin for their support. Thanks also are due to CROMAC for information exchanges and the advices of Prof. Milan Bajic. Finally, we thank Paolo Pasquali and Paolo Riccardi of SARMAP for the processing of SAR data.

Author details

Damien Closson* and Nada Milisavljevic

*Address all correspondence to: damien.closson@yahoo.fr

Eurosense Belfotop, Wemmel, Belgium; European Commission, Brussels, Belgium

References

[1] Bouaraba A, Belhadj-Aissa A, Closson D. Man-made change detection using high-resolution Cosmo-SkyMed SAR Interferometry. Arabian Journal for Science and Engineering January 2016; 41(1) 201–208 DOI: 10.1007/s13369-015-1736-4 .

[2] Massonnet D, Feigl K L. Radar interferometry and its application to changes in the Earth's surface. Reviews of Geophysics 1998; 36(4) 441–500.

[3] Ichoku C, Karnieli A, Arkin Y, Chorowicz J, Fleury T, Rudant J P. Exploring the utility potential of SAR interferometric coherence images. International Journal of Remote Sensing 1998; 19(6) 1147–1160.

[4] Liu J G, Capes R, Haynes M, Moore J McM. ERS SAR multi-temporal coherence image as a tool for sand desert study (dune movement, sand encroachment and erosion). In: Conference Proceedings of the 12th International Conference and Workshop on Applied Geologic Remote Sensing, Denver, Colorado, November 1997, 17–19. (Ann Arbor: ERIM), I-478–485.

[5] Lee H, Liu J G. Spatial decorrelation due to the topography in the interferometric SAR coherence image. In: Conference Proceedings of the International Geoscience and

Remote Sensing Symposium (IGARSS'99), Hamburg, Germany, 28 June–3 July 1999 (Piscataway, NJ: IEEE), 1, 485–487.

[6] Liu J G, Black A, Lee H, Hanaizumi H, Moore J McM. Land surface change detection in a desert area in Algeria using multi-temporal ERS SAR coherence images. International Journal of Remote Sensing 2001; 22(13) 2463–2477.

[7] Manspeizer N, Karnieli A, Arkin Y, Chorowicz J. Analyzing potential cliff erosivity from ERS-SAR satellite imagery. International Journal of Remote Sensing 2001; 22(5) 807–817.

[8] Wegmuller U, Strozzi T, Farr T, Werner C L. Arid land surface characterization with repeat-pass SAR interferometry. IEEE Transactions on Geoscience and Remote Sensing 2000; 38(2) 776–781.

[9] Usai S, Klees R. SAR interferometry on a very long time scale: A study of the interferometric characteristics of man-made features. IEEE Transactions on Geoscience and Remote Sensing 1999; 37(4) 2118–2123.

[10] Usai S. An analysis of the interferometric characteristics of anthropogenic features. IEEE Transactions on Geoscience and Remote Sensing 2000; 38(3) 1491–1497.

[11] Weydahl D J. Analysis of ERS SAR coherence images acquired over vegetated areas and urban features. International Journal of Remote Sensing 2001; 22(14) 2811–2830.

[12] Milisavljević N, Closson D, Bloch I. Detecting human-induced scene changes using coherent change detection in SAR images. In: Proceedings of ISPRS Commission VII Symposium, vol. XXXVIII-7B, pp. 389–394, Vienna, Austria; 2010.

[13] Milisavljević N, Closson D, Bloch I. Detecting potential human activities using coherent change detection. In: Proceedings of the 2nd International Conference on Image Processing Theory Tools and Applications (IPTA), pp. 482–485, Paris, France; 2010.

[14] Closson D. Cooccurrence between the geo-hazards induced by the dead sea level lowering and the geological setting—Lisan Peninsula, Lynch Strait, Ghor Al Haditha, Jordan, University of Liege; 2005.

[15] Milisavljević N, Closson D. Spaceborne Radar Interferometric Techniques for Humanitarian Demining and Land Release. Final Report (unpublished), Belgian Science Policy (Belspo). STEREO II, project SR/20/165 – 30 SPRINT; 41 pages; 2013.

[16] Derauw D. Phase unwrapping using coherence measurements. In: Proceedings of SPIE 2584, Synthetic Aperture Radar and Passive Microwave Sensing, Paris, 21 November, 1995; DOI: 10.1117/12.227141

[17] Seymour M S, Cumming I G. Maximum likelihood estimation for SAR interferometry. Geoscience and Remote Sensing Symposium, Pasadena, California, 1994. IGARSS '94. Surface and Atmospheric Remote Sensing: Technologies, Data Analysis and Interpretation. DOI:10.1109/IGARSS.1994.399711

[18] Bouaraba A. Coherent change detection using high resolution SAR images. PhD thesis, Ecole Militaire Polytechnique/Ecole Royale Militaire; 2014.

[19] Rosen PA, Hensley S, Joughin IR, Li F, Madsen SN, et al. Synthetic aperture radar interferometry. Proceedings of the IEEE 2000; 88(3) 333–382.

[20] Zebker H A, Villasenor J. Decorrelation in interferometric radar echoes. IEEE Transactions on Geoscience and Remote Sensing 1992; 30(5) 950–959.

[21] Ferretti A, Prati C, Rocca F. Permanent scatterers in SAR interferometry. IEEE Transactions on Geoscience and Remote Sensing 2001; 39(1) 8–20.

[22] Berardino P, Fornaro G, Lanari R, Sansosti E. A new algorithm for surface deformation monitoring based on small baseline differential SAR interferograms. IEEE Transactions on Geoscience and Remote Sensing 2002; 40(11) 2375–2383.

[23] Bajić M, Turšič R. Operations with advanced intelligence decision support system for mine suspected area assessment in Croatia and Bosnia and Herzegovina. UNMAS/GICHD Mine Action Technology Workshop; 2010. http://www.gichd.org/fileadmin/GICHD/what-we-do/events/Technology-Workshop-2010/C-6Sept2010-SMART-TechWS.pdf